Spectrochimica Acta Part A: Molecular and Biomolecular Spectroscopy 119 (2014) 84–89

Contents lists available at SciVerse ScienceDirect

Spectrochimica Acta Part A: Molecular and Biomolecular Spectroscopy

journal homepage: www.elsevier.com/locate/saa

Numerically constructed internal-coordinate Hamiltonian with Eckart embedding and its application for the inversion tunneling of ammonia

Csaba Fábri, Edit Mátyus, Attila G. Császár *

Laboratory of Molecular Structure and Dynamics, Institute of Chemistry, Eötvös University, P.O. Box 32, H-1518 Budapest 112, Hungary

HIGHLIGHTS

- Eckart-frame with kinetic energy operators expressed in curvilinear coordinates.
- Utilization of the transformation method of Dymarsky and Kudin.
- Extension of the GENIUSH code: J. Chem. Phys. 130, 134112 (2009); 134, 074105 (2011).
- Determination of rotational–vibrational energy levels and wave functions of ammonia.

GRAPHICAL ABSTRACT

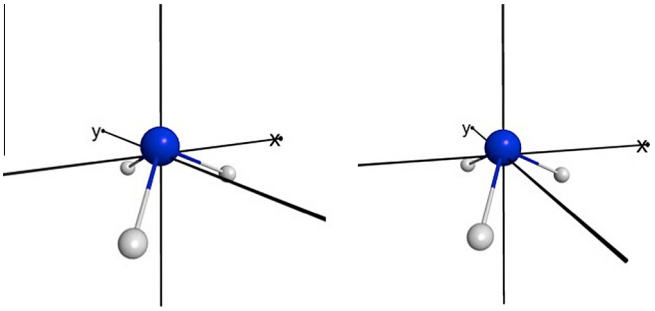

ARTICLE INFO

Article history:
Available online 19 April 2013

Keywords:
Eckart embedding
Ammonia
Nuclear motion computation

ABSTRACT

It is shown that the use of an Eckart-frame embedding with a kinetic energy operator expressed in curvilinear internal coordinates becomes feasible and straightforward to implement for arbitrary molecular compositions and internal coordinates if the operator is defined numerically over a (discrete variable representation) grid. The algorithm proposed utilizes the transformation method of Dymarsky and Kudin to maintain the rotational Eckart condition. In order to demonstrate the applicability and flexibility of our approach the non-rigid ammonia molecule is considered and the corresponding rotational–vibrational energy levels and wave functions are computed using kinetic energy operators with three different embeddings. Two of them fulfill the Eckart conditions corresponding to a trigonal pyramidal (C_{3v}) and a trigonal planar (D_{3h}) reference structure and the third one is a non-Eckart frame. The computed energy levels are, of course, identical, and the structure of the three different wave-function representations are analyzed in terms of the rigid rotor functions for a symmetric top. The possible advantages of one frame representation over another are discussed concerning the interpretation of the rovibrational states in terms of the traditional rigid rotor labels.

1. Introduction

Conditions defining a set of rotating molecule-fixed axes helping to describe vibrations and rotations of semirigid and nonrigid polyatomic molecules are basic to nuclear motion theory [1–3]. It was Eckart [4] who formulated the equations leading to an optimal separation of the two types of motion (yielding zero rotational–vibrational coupling at a reference structure). The translational Eckart condition is

$$\sum_{\alpha=1}^{N} m_\alpha \mathbf{r}_\alpha = \mathbf{0}, \tag{1}$$

where m_α and $\mathbf{r}_\alpha$ stand for the masses and instantaneous position vectors of the N nuclei under examination. This condition keeps the nuclear center of mass at the origin of the body-fixed coordinate system and can be satisfied trivially for arbitrary values of N. The rotational Eckart condition,

$$\sum_{\alpha=1}^{N} m_\alpha (\mathbf{r}_\alpha \times \mathbf{a}_\alpha) = \mathbf{0}, \tag{2}$$

* Corresponding author. Tel.: +36 1 372 2929; fax: +36 1 372 2592.
E-mail address: csaszar@chem.elte.hu (A.G. Császár).

1386-1425/$ - see front matter © 2013 Elsevier B.V. All rights reserved.
http://dx.doi.org/10.1016/j.saa.2013.03.090

where $\mathbf{a}_\alpha$ gives the position of the αth particle in the reference configuration chosen, results in a set of more complex equations. This is the condition which reduces the coupling of vibrations and rotations. Fulfilling the rotational Eckart condition, Eq. (2), can be interpreted as finding a $\mathbf{T}$ (pseudo)rotation matrix which transforms the $\mathbf{r}'_\alpha$ initial position vectors into the $\mathbf{r}_\alpha = \mathbf{T}\mathbf{r}'_\alpha$ position vectors corresponding to the Eckart frame.

Following Eckart [4], Pickett and Strauss [5] derived a procedure for finding the $\mathbf{T}$ transformation matrix. An important shortcoming of the methods of Eckart as well as that of Pickett and Strauss is the need for computing the inverse of an intermediate matrix which can be singular for certain nuclear arrangements. A third method, free of this singularity problem, has recently been introduced by Dymarsky and Kudin [6]. This is the technique utilized in the present study.

As the Eckart frame minimizes the rotational–vibrational coupling, several authors attempted to derive Eckart-embedded kinetic energy operators (KEO) for use in nuclear motion theory, including computational molecular spectroscopy. For rectilinear vibrational coordinates (including normal coordinates), the theory has been worked out by Watson [7,8]. The Eckart–Watson KEO has been successfully applied for nuclear-motion computations of N-atomic molecules in several groups [9–15], including our own [16–18]. However, this KEO is only suitable for treating semirigid molecules. For curvilinear internal coordinates, analytic Eckart formulae and Eckart-embedded KEOs have been derived for triatomic [19–21] as well as more general planar molecules [22,23]. These operators are capable of treating molecules exhibiting arbitrary (either small or large amplitude) motions. Nevertheless, drawbacks of the Eckart-embedded KEOs expressed in internal coordinates are as follows: (a) the operators have a rather complex form, which makes their implementation less desirable, and (b) analytical Eckart KEOs have been derived only for special cases. It is worth noting at this point that flexible reference configurations, as opposed to the choice of a rigid, *e.g.*, equilibrium structure, have been introduced in several spectroscopic models, including the Hougen–Bunker–Johns approach [24] and several of its extensions and variants [25–27]. It is also important to note that the Casimir condition [28,29] provides an alternative expression to minimize the coupling between vibrations and rotations.

In summary, it has remained a challenge to construct general Eckart-embedded KEOs expressed in arbitrary curvilinear coordinates. It is our belief that one particularly useful way forward is to construct the KEO not analytically but numerically, *i.e.*, on a grid. This approach has been followed for quantum chemical computations by several groups [30–36], without considering the Eckart embedding but employing other flexible reference configurations. It should also be mentioned that McCoy and co-workers implemented a numerical Eckart-embedded KEO and used it for the examination of the SO_2 and H_2CO molecules by canonical Van Vleck perturbation theory [37]. Merging the Dymarsky–Kudin scheme with the numerical construction of KEOs is a principal aim of the present study. Another important objective of the present paper is to examine the rovibrational energy levels and wave functions of the flexible NH_3 molecule with the use of Eckart-embedded KEOs. Special emphasis is placed on the analysis of the differences resulting from the choice of the equilibrium (C_{3v}) versus planar (D_{3h}) reference geometries. For this analysis the rigid rotor decomposition (RRD) scheme [38,39] is utilized.

2. Theory

The algorithm GENIUSH (General code with Numerical, Internal-coordinate, User-Specified Hamiltonians) [35,36] provides the starting point of this discussion. In GENIUSH the KEO is constructed numerically and represented on a discrete variable representation (DVR) grid [40]. To set up the KEO in the Eckart embedding it is sufficient to transform the nuclear geometries corresponding to each different grid point into the Eckart frame. To minimize the length of this section the interested reader is referred to the noted publications for details and only the most important novel aspects are discussed below besides the brief summary of the Dymarsky–Kudin scheme.

2.1. Theory of the rotational Eckart condition

The initial step in the method advocated by Dymarsky and Kudin [6] is the definition of a matrix $\mathbf{A}$,

$$A_{ij} = \sum_{\alpha=1}^{N} m_\alpha (\mathbf{r}'_\alpha)_i (\mathbf{a}_\alpha)_j, \quad i,j = 1,2,3, \tag{3}$$

computed with the $\mathbf{r}'_\alpha$ actual and $\mathbf{a}_\alpha$ reference position vectors, where i and j denote Cartesian indices. If a $\mathbf{T}$ pseudorotation ($\mathbf{T}^T = \mathbf{T}^{-1}$) matrix acts on the initial coordinates $\mathbf{r}'_\alpha$ and transforms them into the $\mathbf{r}_\alpha = \mathbf{T}\mathbf{r}'_\alpha$ Eckart coordinates, the elements of the resulting symmetric $\mathbf{S}$ matrix can be expressed as

$$S_{ij} = \sum_{\alpha=1}^{N} m_\alpha (\mathbf{r}_\alpha)_i (\mathbf{a}_\alpha)_j = (\mathbf{TA})_{ij}. \tag{4}$$

The symmetric nature of $\mathbf{S}$ is assured by the rotational Eckart condition, Eq. (2).

The next step is the introduction of the $\mathbf{A}_1 = \mathbf{A}^T\mathbf{A}$ and $\mathbf{A}_2 = \mathbf{A}\mathbf{A}^T$ symmetric matrices, and the solution of the eigenproblems

$$\mathbf{A}_1\mathbf{u}_i = \lambda_i \mathbf{u}_i, \tag{5}$$

and

$$\mathbf{A}_2\mathbf{v}_i = \lambda_i \mathbf{v}_i,$$

where $i = 1, 2, 3$. It can be proved that the eigenvalue sets of $\mathbf{A}_1$ and $\mathbf{A}_2$ coincide. After considering the

$$\mathbf{S}^2 = \mathbf{S}^T\mathbf{S} = \mathbf{A}^T\mathbf{T}^T\mathbf{T}\mathbf{A} = \mathbf{A}_1 \tag{6}$$

and

$$\mathbf{S}^2 = \mathbf{S}\mathbf{S}^T = \mathbf{T}\mathbf{A}\mathbf{A}^T\mathbf{T}^T = \mathbf{T}\mathbf{A}_2\mathbf{T}^T \tag{7}$$

relations, we get

$$\mathbf{A}_1\mathbf{T} = \mathbf{T}\mathbf{A}_2. \tag{8}$$

Therefore, the $\mathbf{T}$ transformation matrix can be constructed according to the

$$\mathbf{T} = \sum_{i=1}^{3} \mathbf{u}_i \circ \mathbf{v}_i \tag{9}$$

formula, where $\mathbf{u}_i$ and $\mathbf{v}_i$ share the same λ_i eigenvalue for $i = 1, 2, 3$. Except for special cases there are eight different $\mathbf{T}$ transformation matrices differing in the relative signs of the $\mathbf{u}_i$ and $\mathbf{v}_i$ eigenvectors. Dymarsky and Kudin [6] suggested the use of the

$$\mathbf{u}_i \cdot \mathbf{v}_i \geqslant 0, \tag{10}$$

with $i = 1, 2, 3$, and

$$\begin{aligned} \mathbf{u}_3 &= \mathbf{u}_1 \times \mathbf{u}_2 \\ \mathbf{v}_3 &= \mathbf{v}_1 \times \mathbf{v}_2 \end{aligned} \tag{11}$$

conditions to find the $\mathbf{T}$ transformation matrix which is closest to the identity matrix and represents a pure rotation ($\det\mathbf{T} = 1$).

2.2. Construction of the Eckart-embedded kinetic energy operator

The general form of the rotational–vibrational Hamiltonian of a molecule with D vibrational degrees of freedom can be written as [35,36]

$$\widehat{H} = \frac{1}{2}\sum_{k=1}^{D+3}\sum_{l=1}^{D+3}\tilde{g}^{-1/4}\hat{p}_k^{\dagger}G_{kl}\tilde{g}^{1/2}\hat{p}_l\tilde{g}^{-1/4} + \widehat{V}, \tag{12}$$

where $\tilde{g} = \det(\mathbf{g})$, $\mathbf{G} = \mathbf{g}^{-1}$, the $\hat{p}_k$ operators are the quasi-momenta and $\widehat{V}$ is the potential energy operator. GENIUSH uses either the matrix representation of the Podolsky form or a more commonly used rearranged form [35]. Although the direct usage of the Podolsky form implies the insertion of a larger number of truncated resolutions of identity during the construction of the matrix representation of the KEO, it requires the evaluation of only the first derivatives of the body-fixed Cartesian coordinates with respect to the internal coordinates, which is a clear advantage of this representation. In this work we used the Podolsky form, because the truncated resolutions of identity and thus the matrix representation of the numerical KEO were found to be appropriate and accurate enough in the vibrational basis set employed. The KEO expressed in internal coordinates needs the

$$g_{ij} = \sum_{\alpha=1}^{N} m_\alpha \frac{\partial \mathbf{r}_\alpha^{\mathrm{T}}}{\partial q_i}\frac{\partial \mathbf{r}_\alpha}{\partial q_j} \tag{13}$$

matrix elements of the well-known $\mathbf{g}$ matrix [41] expressed in terms of the $3N-3$ q_i generalized ($3N-6$ vibrational and 3 rotational) coordinates.

Within the framework of GENIUSH, the $\mathbf{g}$ matrix is evaluated by the numerical computation of the so-called $\mathbf{t}$-vectors, $\frac{\partial \mathbf{r}_\alpha}{\partial q_i}$, by the method of central differences at the $(q_1,\ldots,q_D)$ DVR grid points given in arbitrary internal coordinates. For that we take finite steps in the selected q_i internal coordinate and compute the Eckart-embedded Cartesian nuclear position vectors for the internal coordinate sets $(q_1,\ldots,q_i+\epsilon/2,\ldots,q_D)$ and $(q_1,\ldots,q_i-\epsilon/2,\ldots,q_D)$, respectively. This is done according to the following procedure: (a) computation of the initial $\mathbf{r}'_\alpha(q_1,\ldots,q_i+\epsilon/2,\ldots,q_D)$ and $\mathbf{r}'_\alpha(q_1,\ldots,q_i-\epsilon/2,\ldots,q_D)$ Cartesian coordinates with respect to an arbitrary initial embedding, (b) shifting the origin into the nuclear center of mass, and (c) transformation of the nuclear position vectors into the $\mathbf{r}_\alpha(q_1,\ldots,q_i+\epsilon/2,\ldots,q_D)$ and $\mathbf{r}_\alpha(q_1,\ldots,q_i-\epsilon/2,\ldots,q_D)$ Eckart coordinates by the previously described method. The Eckart-embedded $\mathbf{t}$-vectors are computed as

$$\frac{\partial \mathbf{r}_\alpha}{\partial q_i}(q_1,\ldots,q_D) = \frac{\mathbf{r}_\alpha(q_1,\ldots,q_i+\epsilon/2,\ldots,q_D) - \mathbf{r}_\alpha(q_1,\ldots,q_i-\epsilon/2,\ldots,q_D)}{\epsilon}. \tag{14}$$

The implementation of this transformation within the GENIUSH protocol presented no significant difficulties. The only pitfall during the numerical construction of the Eckart-embedded $\mathbf{t}$-vectors is the possible instability of the numerical differentiation. If two slightly different initial $\mathbf{r}'_\alpha$ vectors, generated by an incremental and a decremental displacement in terms of an internal coordinate, are not transformed by the same subcase of the eight possible Eckart transformations, the resulting $\mathbf{t}$-vector will be erroneous. Thus, to assure the stability of the numerical differentiation, the same Eckart subcase must be selected for the two vectors mentioned. To achieve this, the criteria represented by Eqs. (10) and (11) are maintained within the GENIUSH program.

Finally we note that any of the possible sign combinations for $\mathbf{u}_i$ and $\mathbf{v}_i$ could be selected for the construction of a (pseudo)rotation $\mathbf{T}$ matrix to obtain Eckart Cartesian coordinates. As long as the same convention is used during the course of a computation the correct rovibrational eigenvalues and eigenvectors are obtained.

2.3. The rigid rotor decomposition (RRD) approach

The rigid rotor decomposition (RRD) [38,39] approach is a tool for the interpretation of variationally computed rovibrational energy levels and wave functions. The initial step is the evaluation of

$$\langle \Psi_i | \phi_j R_k \rangle \tag{15}$$

overlap integrals, where Ψ_i is the rovibrational wave function to be labelled by either exact or approximate vibrational and rotational quantum numbers, while ϕ_j and R_k denote variationally determined vibrational and rigid-rotor wave functions, respectively. After finding the dominant $\phi_a R_b$ contribution in Ψ_i, it is straightforward to label Ψ_i with the vibrational labels of ϕ_a and the rotational labels of R_b.

3. Computational details

As one of the objectives of the present study is the examination of the effect of the choice of the body-fixed frame on the determination of the rovibrational energy levels and wave functions for the flexible NH_3 molecule, these have been computed with the GENIUSH program with three different embeddings. To start with, Eckart frames with C_{3v} (equilibrium) and D_{3h} (planar) point-group symmetry reference structures (see Table 1) have been utilized. Furthermore, we employed a non-Eckart frame (called 'traditional' (trad.) frame henceforth) defined as follows: (a) the origin of the body-fixed frame is placed on the first atom (N); (b) the z axis is directed toward the second atom (X, a dummy atom); (c) the xz plane is defined by the first three atoms (N, X, and H_1); (d) the y axis is oriented according to the right-hand rule; and (e) the origin is shifted to the center of mass of the nuclei. The RRD computations utilized symmetric top eigenfunctions for all the embeddings as the NH_3 molecule is a symmetric top.

The PES of NH_3 employed in this study is taken from Ref. [42]. It corresponds to the PES called spectroscopic in that study. Atomic masses, $m_H = 1.007825$ u and $m_N = 14.003074$ u, were employed throughout the nuclear motion computations. The set of internal coordinates chosen for the rotational–vibrational computations is summarized in Table 2. According to Ref. [35], we used the stepsize $\epsilon = 10^{-5}$ for the numerical evaluation of the $\mathbf{t}$-vectors. Our computational studies have employed the six-dimensional (active inversion, 6D) and the three-dimensional stretch-only reduced dimensional (inactive inversion, 3D) computational models. In the case of the 3D stretch-only model values of the constrained angle coordinates were fixed at their equilibrium values

Table 1
Cartesian coordinates, in Å, of the C_{3v} and D_{3h} Eckart reference structures used in this work.

α	Eckart (C_{3v})			Eckart (D_{3h})		
	$(\mathbf{a}_\alpha)_x$	$(\mathbf{a}_\alpha)_y$	$(\mathbf{a}_\alpha)_z$	$(\mathbf{a}_\alpha)_x$	$(\mathbf{a}_\alpha)_y$	$(\mathbf{a}_\alpha)_z$
N	0.0	0.0	0.067544	0.0	0.0	0.0
H_1	0.936899	0.0	−0.312826	0.994378	0.0	0.0
H_2	−0.468449	−0.811378	−0.312826	−0.497189	−0.861157	0.0
H_3	−0.468449	0.811378	−0.312826	−0.497189	0.861157	0.0

Table 2
Z-matrix representation of the internal coordinates of NH_3. Symbol X refers to a dummy atom.

N						
X	N	1.0				
H_1	N	r_1	X	θ		
H_2	N	r_2	X	θ	H_1	β_1
H_3	N	r_3	X	θ	H_1	$-\beta_2$

$\beta_1 = \beta_2 = 120°$ and $\theta = 106.36°$. Besides the pure vibrational energy levels and wave functions rovibrational energy levels and wave functions for the first ten vibrational states were computed by GENIUSH for rotational quantum numbers $J = 1$ and 2 with the 6D and 3D models. In the case of the 6D model 25 and 8 Hermite-DVR basis functions have been employed for the θ inversion and the other vibrational coordinates, respectively; thus, the overall size of the vibrational basis equals 25×8^5. For the 3D model 30 Hermite-DVR basis functions for each of the active vibrational coordinates have been utilized resulting in a vibrational basis of dimension 30^3. For each internal coordinate these Hermite-DVR basis functions were generated by potential optimization done in the basis of 80 primitive Hermite-DVR functions. We found that this basis allowed the insertion of approximate resolutions of identity among the different operators present in the KEO; thus, the Podolsky form of the general rovibrational KEO can be applied in a straightforward manner.

For testing the convergence of the computed results we also used some auxiliary basis sets of size 20×6^5, 30×10^5 (6D), and 35^3 (3D). Based on these tests we can conclude that energy levels reported in this study are converged to 0.01 cm^{-1} or better, whereas RRD coefficients given in Tables 3 and 4 are converged to a few 0.0001 units.

4. Results and discussion

In this section we demonstrate the applicability of the numerically constructed KEO using the Eckart embedding and internal coordinates in a variational procedure. Using the GENIUSH program we solve the internal-coordinate rovibrational Schrödinger equation with Eckart embedding for a more than three-particle system for the first time. To challenge our implementation we chose the ammonia molecule as an example and are aiming to describe its famous inversion tunneling with a full rovibrational model using a trigonal pyramidal (C_{3v}) Eckart reference structure. Since we can easily switch between different body-fixed frames in the GENIUSH program, we also run computations with a trigonal planar Eckart reference structure of D_{3h} symmetry. This Eckart embedding is known to provide a working model for the ammonia inversion with the Eckart–Watson Hamiltonian as well [43,44], in contrast to the equilibrium C_{3v} reference structure. In addition to these two Eckart frames we use a 'traditional' embedding. Besides the demonstration of the flexibility and applicability of our numerical approach for various embeddings including the challenging Eckart one, we also compare the numerical results corresponding to the three different numerically constructed rovibrational Hamiltonians.

The converged energy levels are, of course, identical for the different KEOs. Furthermore, for both the 3D and 6D models the convergence rate of the rovibrational energy levels was similar for all the embeddings. What is more interesting is the structure of the rotational–vibrational wave function representation, which can be analysed by inspecting the RRD coefficients. In what follows, we collect our major observations for the RRD analysis in the hope that one or the other representations of the KEO facilitates the interpretation of the calculated rovibrational states in terms of the conventional rigid rotor labels.

Results of the RRD analysis of the rotational–vibrational states computed with different body-fixed frame embeddings (for the 6D and 3D models) are summarized in Tables 3 and 4 for $J = 1$

Table 3
Absolute values of the dominant net RRD coefficients, Eq. (16), for the 6D rovibrational model of NH_3. The rovibrational energy levels shown in this table belong to the selected ν_2^+ (932.48 cm^{-1}, A_1' symmetry) and ν_4^- (1627.29 cm^{-1}, E'' symmetry) vibrational band origins and are referenced to the zero-point vibrational energy level (7430.28 cm^{-1}). J denotes the total angular momentum quantum number and K is the absolute value of the projection of the total angular momentum on the molecule-fixed z axis. The designations Eckart (C_{3v}), Eckart (D_{3h}) and 'trad.' stand for the Eckart frames with C_{3v} (equilibrium) and D_{3h} (planar) point-group symmetry reference structures, and for the 'traditional' frame, respectively. Energy levels corresponding to irreducible representations A_1' and A_1'' are unfeasible due to the fermionic nature of protons and they are listed here only for the sake of completeness.

E/cm^{-1}	Γ_{rve}	VBO	J	K	RRD coefficients		
					Eckart (C_{3v})	Eckart (D_{3h})	trad.
948.64	E''	ν_2^+	1	1	0.9978	0.9994	0.9951
948.64		ν_2^+	1	1	0.9978	0.9994	0.9952
952.62	A_2'	ν_2^+	1	0	0.9957	0.9988	0.9992
1640.54	E'	ν_4^-	1	1	0.9960	0.9988	0.9900
1640.54		ν_4^-	1	1	0.9960	0.9988	0.9898
1646.33	A_1'	ν_4^-	1	1	0.9989	0.9997	0.9906
1647.16	A_2'	ν_4^-	1	1	0.9885	0.9935	0.9847
1647.69	E''	ν_4^-	1	0	0.9905	0.9962	0.9967
1647.69		ν_4^-	1	0	0.9905	0.9962	0.9967
976.96	E'	ν_2^+	2	2	0.9957	0.9984	0.9814
976.96		ν_2^+	2	2	0.9957	0.9984	0.9814
988.88	E''	ν_2^+	2	1	0.9892	0.9970	0.9934
988.88		ν_2^+	2	1	0.9892	0.9970	0.9937
992.85	A_1'	ν_2^+	2	0	0.9871	0.9964	0.9976
1666.16	A_2''	ν_4^-	2	2	0.9921	0.9977	0.9621
1666.16	A_1''	ν_4^-	2	2	0.9923	0.9978	0.9622
1678.50	E''	ν_4^-	2	2	0.9877	0.9871	0.9514
1678.50		ν_4^-	2	2	0.9876	0.9871	0.9517
1681.37	E'	ν_4^-	2	1	0.9780	0.9918	0.9843
1681.37		ν_4^-	2	1	0.9779	0.9917	0.9837
1686.40	A_2'	ν_4^-	2	1	0.9893	0.9971	0.9890
1688.64	E''	ν_4^-	2	0	0.9724	0.9830	0.9847
1688.64		ν_4^-	2	0	0.9721	0.9830	0.9848
1688.88	A_1'	ν_4^-	2	1	0.9725	0.9793	0.9720

Table 4
Absolute values of the dominant net RRD coefficients, Eq. (16), for the 3D stretch-only rovibrational model of NH_3. The rovibrational energy levels shown in this table belong to the selected ν_1 (3390.93 cm^{-1}, A_1 symmetry) and ν_3 (3567.56 cm^{-1}, E symmetry) vibrational band origins (VBO) and are referenced to the zero-point vibrational energy level (5783.63 cm^{-1}). J denotes the total angular momentum quantum number and K is the absolute value of the projection of the total angular momentum on the molecule-fixed z axis. The designations Eckart (C_{3v}), Eckart (D_{3h}) and 'trad.' stand for the Eckart frames with C_{3v} (equilibrium) and D_{3h} (planar) point-group symmetry reference structures and for the 'traditional' frame, respectively.

E/cm^{-1}	Γ_{rve}	VBO	J	K	RRD coefficients		
					Eckart (C_{3v})	Eckart (D_{3h})	trad.
3406.86	E	ν_1	1	1	1.0000	0.9999	1.0000
3406.86		ν_1	1	1	1.0000	0.9999	1.0000
3411.25	A_2	ν_1	1	0	1.0000	0.9998	1.0000
3582.59	E	ν_3	1	1	0.9999	0.9998	0.9999
3582.59		ν_3	1	1	0.9999	0.9998	0.9999
3583.87	A_2	ν_3	1	1	1.0000	0.9996	1.0000
3584.29	A_1	ν_3	1	1	1.0000	1.0000	1.0000
3587.72	E	ν_3	1	0	0.9999	0.9996	0.9999
3587.72		ν_3	1	0	0.9999	0.9996	0.9999
3434.34	E	ν_1	2	2	1.0000	0.9998	1.0000
3434.34		ν_1	2	2	1.0000	0.9998	1.0000
3447.50	E	ν_1	2	1	0.9999	0.9995	1.0000
3447.50		ν_1	2	1	0.9999	0.9995	1.0000
3451.89	A_1	ν_1	2	0	0.9999	0.9994	1.0000
3609.02	A_2	ν_3	2	2	0.9998	0.9995	0.9998
3609.02	A_1	ν_3	2	2	0.9998	0.9995	0.9998
3611.98	E	ν_3	2	2	0.9994	0.9991	0.9977
3611.98		ν_3	2	2	0.9994	0.9991	0.9977
3622.90	E	ν_3	2	1	0.9997	0.9989	0.9997
3622.90		ν_3	2	1	0.9997	0.9989	0.9997
3623.76	A_1	ν_3	2	1	0.9997	0.9983	0.9998
3625.02	A_2	ν_3	2	1	0.9998	0.9995	0.9998
3628.04	E	ν_3	2	0	0.9991	0.9982	0.9988
3628.04		ν_3	2	0	0.9991	0.9982	0.9988

and $J = 2$, respectively. NH_3 is a symmetric-top molecule and it has one- and two-fold degenerate vibrational band origins (VBOs). It is thus worth introducing four RRD cases defined by the properties of the vibrational and rigid-rotor functions of the dominant RRD subspace: (a) one-fold degenerate VBO with $K = 0$; (b) one-fold degenerate VBO with $K \neq 0$; (c) two-fold degenerate VBO with $K = 0$; and (d) two-fold degenerate VBO with $K \neq 0$, where $K = |k|$ and k is the projection of the total angular momentum on the molecule-fixed z axis. Rigid-rotor states sharing the same K value are degenerate; thus, for cases (a), (b), (c), and (d) the dimension of the corresponding RRD subspaces are one, two, two, and four, respectively. For a given RRD subspace the net RRD coefficient can be defined as

$$\sqrt{\sum_{j=1}^{n}\sum_{k\in\{K,-K\}}|\langle\Psi_i|\phi_j R_k\rangle|^2} \tag{16}$$

for an n-fold degenerate VBO (*i.e.*, the ϕ_j vibrational eigenfunctions have the same eigenvalue) and for either one-fold ($K = 0$) or two-fold ($K \neq 0$) degenerate R_k rigid-rotor functions. After finding the dominant net RRD coefficient one can assign n ($K = 0$) or $2n$ ($K \neq 0$) Ψ_i rotational–vibrational states with the vibrational quantum numbers of the n-fold degenerate VBO and the K value of the rigid-rotor function(s). Finally, it is important to note that variational rotational–vibrational states of NH_3 assigned with a two-fold degenerate VBO and $K \neq 0$ are not four-fold degenerate, as the D_{3h}(M) molecular symmetry group [3] contains only one- and two-dimensional irreducible representations.

In the case of the 6D model, rovibrational states associated with the ν_2^+ (932.48 cm^{-1}) and ν_4^- (1627.29 cm^{-1}) VBOs are presented in Table 3. For the ν_2^+ VBO, we get one-fold and two-fold degenerate rovibrational states for $K = 0$ and $K \neq 0$ values, respectively. For the ν_4^- VBO of E'' symmetry, rovibrational levels with $K = 0$ values exhibit two-fold degeneracies, while for $K \neq 0$ quantum numbers the corresponding four rovibrational levels are split according to a 2 + 1 + 1 pattern. In the 6D model the inversion of NH_3 is active and for the majority of the examined rovibrational states the D_{3h} Eckart embedding slightly outperforms the other two in terms of the largest dominant net RRD coefficient. Clearly, the 'traditional' embedding results in the smallest dominant RRD coefficients. This result is similar to that obtained during a similar study for $H_2^{16}O$ [39]. Nevertheless, that study also showed that beyond a certain excitation energy and J quantum number the Eckart embedding will also fail to provide a dominant RRD coefficient larger than 0.7 and thus it is not significantly better than the traditional embedding. The $K = 0$ results color this picture somewhat in that it is the 'traditional' embedding that results in the largest RRD coefficients. This is a somewhat counterintuitive result and we cannot offer an explanation for it.

For the 3D model rovibrational states associated with the ν_1 (3390.93 cm^{-1}, A_1 symmetry) and ν_3 (3567.56 cm^{-1}, E symmetry) VBOs are given in Table 4. Here the same symmetry and splitting considerations hold for the rovibrational states, the only difference is that the C_{3v}(M) molecular symmetry group is used instead of D_{3h}(M). In this case the inversion of NH_3 is inactive, and the C_{3v} Eckart and 'traditional' embeddings give dominant net RRD contributions of similar quality for most of the rovibrational states examined by us, while the D_{3h} Eckart embedding performs slightly worse than the other two.

Generally, for both the 6D and 3D models, differences between the three embeddings in terms of the absolute value of the dominant net RRD coefficients are found to be negligible, and the RRD-based assignment procedure has been successful for all the examined rovibrational states. However, for increasing rovibrational excitations, differences in the RRD analysis between the different embeddings become more pronounced. Based on these arguments and our results, for models exhibiting active inversion the D_{3h} Eckart frame, and for models without inversion, the C_{3v} Eckart frame seem to be more adequate.

5. Summary

It is shown in this paper that the use of a general Eckart-embedded kinetic energy operator (KEO), expressed in arbitrary curvilinear coordinates, becomes possible if the KEO is constructed numerically and represented on a (discrete variable representation (DVR)) grid. This new approach exhibits the following significant advantages: (a) applicability to arbitrary internal coordinates and molecular compositions, and (b) no complicated analytical derivations are required. The implementation of Eckart-embedded KEOs expressed in arbitrary internal coordinates presented no significant difficulties within our in-house GENIUSH program.

This study employed the flexible NH_3 molecule as a test case for comparing rotational–vibrational energy levels and wave functions computed with and without the use of Eckart-embedded KEOs. For the 6D and the 3D stretch-only models of NH_3 we executed variational rotational–vibrational computations with 'traditional' and Eckart (utilizing reference geometries of C_{3v} and D_{3h} point-group symmetries) body-fixed frame embeddings. The rigid rotor decomposition (RRD) analysis of the rotational–vibrational states of NH_3 showed no substantial differences between the three embedding choices and the RRD-based labeling procedure has been successful for all the examined rovibrational states. However, based on the results of this study, for models exhibiting active inversion (6D model in this case) the D_{3h} Eckart frame, and for models without inversion (3D model), the C_{3v} Eckart frame was found to be more adequate.

To supplement the results of the present paper we can recall some of the relevant results of our previous study [39] employing basically the same approach for $H_2^{16}O$, whereby much higher rovibrational states with much higher J values were studied employing several embeddings. That study clearly proved that while at low excitation the Eckart embedding outperforms the 'traditional' ones, above some excitation level either in the vibrations or the rotations even the Eckart embedding does not ensure a clear separation of vibrations and rotations, as evidenced by the lack of a dominant RRD coefficient and an overly heavy mixing of basis states.

Acknowledgments

This work was supported by an ERA-Chemistry Grant and by the Hungarian Scientific Research Fund (OTKA, Grant No. NK83583). The authors are grateful to Professors Brian T. Sutcliffe and Tucker Carrington for useful discussions.

References

[1] M. Born, W. Heisenberg, Ann. Phys. 379 (1924) 1.
[2] J.D. Louck, H.W. Galbraith, Rev. Mod. Phys. 48 (1976) 69.
[3] P.R. Bunker, P. Jensen, Molecular Symmetry and Spectroscopy, NRC, Ottawa, 1998.
[4] C. Eckart, Phys. Rev. 47 (1935) 552.
[5] H.M. Pickett, H.L. Strauss, J. Am. Chem. Soc. 92 (1970) 7281.
[6] A.Y. Dymarsky, K.N. Kudin, J. Chem. Phys. 122 (2005) 124103.
[7] J.K.G. Watson, Mol. Phys. 15 (1968) 479.
[8] J.K.G. Watson, Mol. Phys. 19 (1970) 465.
[9] G.D. Carney, L.I. Sprandel, C.W. Kern, Adv. Chem. Phys. 37 (1978) 305.
[10] S. Carter, J.M. Bowman, N.C. Handy, Theor. Chem. Acc. 100 (1998) 191.
[11] J.M. Bowman, S. Carter, X. Huang, Int. Rev. Phys. Chem. 22 (2003) 533.
[12] G. Rauhut, J. Chem. Phys. 121 (2004) 9313.
[13] O. Christiansen, Phys. Chem. Chem. Phys. 9 (2007) 2942.
[14] I. Scivetti, J. Kohanoff, N. Gidopoulos, Phys. Rev. A 79 (2009) 032516.
[15] I. Scivetti, J. Kohanoff, N. Gidopoulos, Phys. Rev. A 80 (2009) 022516.
[16] E. Mátyus, G. Czakó, B.T. Sutcliffe, A.G. Császár, J. Chem. Phys. 127 (2007) 084102.
[17] E. Mátyus, J. Šimunek, A.G. Császár, J. Chem. Phys. 131 (2009) 074106.

[18] C. Fábri, E. Mátyus, T. Furtenbacher, B. Mihály, T. Zoltáni, L. Nemes, A.G. Császár, J. Chem. Phys. 135 (2011) 094307.
[19] H. Wei, T. Carrington, J. Chem. Phys. 107 (1997) 2813.
[20] H. Wei, T. Carrington, J. Chem. Phys. 107 (1997) 9493.
[21] H. Wei, T. Carrington, Chem. Phys. Lett. 287 (1998) 289.
[22] H. Wei, J. Chem. Phys. 118 (2003) 7202.
[23] H. Wei, J. Chem. Phys. 118 (2003) 7208.
[24] J.T. Hougen, P.R. Bunker, J.W.C. Johns, J. Mol. Spectrosc. 34 (1970) 136.
[25] V. Spirko, J. Mol. Spectrosc. 101 (1983) 30.
[26] V. Szalay, J. Mol. Spectrosc. 128 (1988) 24.
[27] S.N. Yurchenko, M. Carvajal, P. Jensen, H. Lin, J. Zheng, W. Thiel, Mol. Phys. 103 (2005) 359.
[28] H.B.G. Casimir, PhD Thesis, University of Leiden, 1931.
[29] K.L. Mardis, E.L. Silbert III, J. Chem. Phys. 106 (1997) 6618.
[30] D. Lauvergnat, A. Nauts, J. Chem. Phys. 116 (2002) 8560.
[31] S.N. Yurchenko, W. Thiel, P. Jensen, J. Mol. Spectrosc. 245 (2007) 126.
[32] D. Luckhaus, J. Chem. Phys. 113 (2000) 1329.
[33] D. Strobusch, Ch. Scheurer, J. Chem. Phys. 135 (2011) 124102.
[34] D. Strobusch, Ch. Scheurer, J. Chem. Phys. 135 (2011) 144101.
[35] E. Mátyus, G. Czakó, A.G. Császár, J. Chem. Phys. 130 (2009) 134112.
[36] C. Fábri, E. Mátyus, A.G. Császár, J. Chem. Phys. 134 (2011) 074105.
[37] A.B. McCoy, D.C. Burleigh, E.L. Sibert, J. Chem. Phys. 95 (1991) 7449.
[38] E. Mátyus, C. Fábri, T. Szidarovszky, G. Czakó, W.D. Allen, A.G. Császár, J. Chem. Phys. 133 (2010) 034113.
[39] T. Szidarovszky, C. Fábri, A.G. Császár, J. Chem. Phys. 136 (2012) 174112.
[40] D.O. Harris, G.G. Engerholm, W.D. Gwinn, J. Chem. Phys. 43 (1965) 1515.
[41] E.B. Wilson, J.C. Decius, P.C. Cross, Molecular Vibrations, McGraw-Hill, New York, 1955.
[42] S.N. Yurchenko, R.J. Barber, J. Tennyson, W. Thiel, P. Jensen, J. Mol. Spectrosc. 268 (2011) 123.
[43] C. Léonard, N.C. Handy, S. Carter, J.M. Bowman, Spectrochim. Acta A 58 (2002) 825.
[44] E. Kamarchik, Y. Wang, J. Bowman, J. Phys. Chem. A 113 (2009) 7556.